Journal of Biomedical Optics

BiomedicalOptics.SPIEDigitalLibrary.org

Determination of continuous complex refractive index dispersion of biotissue based on internal reflection

Zhichao Deng
Jin Wang
Qing Ye
Tengqian Sun
Wenyuan Zhou
Jianchun Mei
Chunping Zhang
Jianguo Tian

SPIE.

Determination of continuous complex refractive index dispersion of biotissue based on internal reflection

Zhichao Deng,[a] Jin Wang,[a] Qing Ye,[a,*] Tengqian Sun,[a] Wenyuan Zhou,[a] Jianchun Mei,[b] Chunping Zhang,[a] and Jianguo Tian[a,*]
[a]Nankai University, Key Laboratory of Weak Light Nonlinear Photonics, Ministry of Education, TEDA Applied Physics School and School of Physics, Tianjin 300071, China
[b]Nankai University, Advanced Technology Institute, Tianjin 300071, China

Abstract. The complex refractive index dispersion (CRID), which contains the information on the refractive index dispersion and extinction coefficient spectra, is an important optical parameter of biotissue. However, it is hard to perform the CRID measurement on biotissues due to their high scattering property. Continuous CRID measurement based on internal reflection (CCRIDM-IR) is introduced. By using a lab-made apparatus, internal reflectance spectra of biotissue samples at multiple incident angles were detected, from which the continuous CRIDs were calculated based on the Fresnel formula. Results showed that in 400- to 750-nm range, hemoglobin solution has complicated dispersion and extinction coefficient spectra, while other biotissues have normal dispersion properties, and their extinction coefficients do not vary much with different wavelengths. The normal dispersion can be accurately described by several coefficients of dispersion equations (Cauchy equation, Cornu equation, and Conrady equation). To our knowledge, this is the first time that the continuous CRID of scattering biotissue over a continuous spectral region is measured, and we hereby have proven that CCRIDM-IR is a good method for continuous CRID research of biotissue. [DOI: 10.1117/1.JBO.21.1.015003]

Keywords: optical parameters; complex refractive index dispersion; extinction coefficient spectra; dispersion coefficients; internal reflection.

Paper 150572R received Aug. 29, 2015; accepted for publication Dec. 8, 2015; published online Jan. 11, 2016.

1 Introduction

Since light propagation in materials is highly related to their optical properties, knowledge about the biotissue's optical parameters is essential for optical diagnostics and optical treatments. Among the parameters, the complex refractive index (CRI) is an important one, which is defined as $n = n_r(1 + i\kappa)$[1]; in some literatures it is defined as $n = n_r + ik$,[2] but here we chose the former form. Because the components in biotissue are complicated, the real part n_r is always known as the effective or average refractive index (RI). The extinction coefficient κ satisfies $n_r\kappa = \mu_t\lambda/4\pi$. The total interaction coefficient μ_t means the energy loss per unit at a certain direction caused by absorption and scattering, and $\mu_t = \mu_a + \mu_s$.[3] Thus, κ can characterize the optical transparency of biotissue. Over the last decades, researchers have developed various methods to determine the n_r of biotissue, such as the optical fiber cladding method,[4] the minimum deviation angle method,[5,6] optical coherent tomography,[7] and the total internal reflection method.[8–12] The inverse adding-double method or the inverse Monte Carlo simulation method are common approaches to determine μ_a and μ_s.[3,12–14] However, simultaneously determining n_r and κ remains a challenge.

As it is known that the optical properties are always wavelength-dependent; investigation of CRI over a wide spectral region is necessary. The dispersion of CRI (CRID), which contains the information of both the refractive index dispersion (RID) and the wavelength-dependent κ, is worth investigating. For a material with normal dispersion, its RID can be described by a dispersion equation with several coefficients. In the literature, the coefficients of biotissue are often deduced from quite few n_r values at discrete wavelengths; for instance, Ding et al.[2] and Cheng et al.[15] measured the n_r at eight and four wavelengths, respectively. Discrete n_r measurement may miss some important information around the absorption peak, such as in our early study of bacteriorhodopsin film.[8] In order to determine the coefficients more accurately, continuous n_r measurement is necessary. To our knowledge, however, no research has been reported on the continuous CRID of biotissue with scattering in a continuous spectral region.

In this study, continuous CRID measurement based on internal reflection (CCRIDM-IR) is introduced. The CCRIDM-IR utilizes a previously proposed lab-made apparatus[16] to detect the angle-dependent internal reflection spectra at the prism–sample interface. Combined with the reflection spectra of air, the angle-dependent internal reflectance spectra of the sample can be detected, from which the continuous CRID can be calculated based on the Fresnel formula. The continuous CRID of methyl red (MR) solution and several kinds of biotissue were measured in the spectral region from 400 to 750 nm. Dispersion coefficients of the biotissues based on dispersion equations were also obtained with perfect fittings. In addition, comparisons were made between our results and the ones reported in the previous literatures.

*Address all correspondence to: Qing Ye, E-mail: yeqing@nankai.edu.cn; Jianguo Tian, E-mail: jjtian@nankai.edu.cn

1083-3668/2016/$25.00 © 2016 SPIE

2 Materials and Method

2.1 *Materials*

In total, 13 different samples were investigated in this study: MR cyclohexanone solution with weight fraction of 0.5%, oxygenated hemoglobin (HbO_2) solution (320 g/l), deoxygenated hemoglobin (Hb) solution (320 g/l), chicken liver, porcine liver, porcine muscle, porcine adipose, bovine muscle, mutton muscle, egg yolk, egg white, animal oil, and biotissue fluid.

MR is a kind of biological stain and has strong absorption in the visual spectra region. Its solution has relatively stable optical parameters. MR powder was dissolved in cyclohexanone liquid to obtain MR solution. Hemoglobin is the main component of blood cells and also an absorptive material. The preparation procedures of Hb and HbO_2 solutions were same as that described in Ref. 17. In simple terms, the lyophilized powder of bovine hemoglobin (Sigma-Aldrich Co. Ltd.) was dissolved in phosphate-buffered saline to maintain pH at 7.4, and then 10 g/l sodium dithionite and 15 g/l sodium bicarbonate solutions were added to obtain Hb and HbO_2 solutions, respectively. The dissolution process was performed three times to obtain three solution samples.

During transportation, the fresh biotissues were preserved at about 0°C. Before measurement, each biotissue was cut into three pieces, and each piece was about 30×40 mm^2 with a thickness of 20 mm. Air gaps at the interface should be avoided when attaching the biotissue sample to the prism. Animal oil was derived from porcine adipose by heating, and biotissue fluid was derived from the bovine muscle by pressing. The amount of oil and fluid were enough for three measurements. Three egg yolk samples and three egg white samples were from three different eggs. The liquid samples, such as animal oil, biotissue fluid, egg yolk, and egg white, were poured into the cell attached to the prism. All measurements were performed until the sample reached room temperature (about 20°C). During the measurements, samples were sealed with preservative film. All experiments on animals followed the ethical principles and standards.

2.2 *Method*

A top-down view of the lab-made apparatus is shown in Fig. 1; it is similar to the one reported in Ref. 16. After passing through a fiber, a beam expander, and an aperture (diameter: 1.5 mm), the light beam from a xenon lamp is parallelized and narrowed. Then it propagates along the direction of the radius of a semicylindrical prism and illuminates the sample attached to the prism. A fiber spectrometer (HR4000, Ocean Optics) is used to detect the reflected beam expanded by a concave lens ($f = -50$ mm).

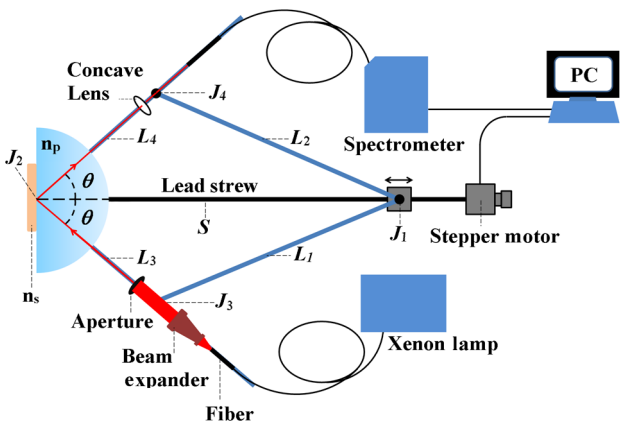

Fig. 1 The lab-made experimental apparatus.

Four arms labeled L_1, L_2, L_3, and L_4 are connected by intersection points J_1, J_2, J_3, and J_4, where J_3 and J_4 are symmetrical about the line J_1J_2. J_1 fixed on a slider that can move along the lead screw, S, driven by a stepper motor. J_2 coincides with the semicircular arc center of the prism, and J_1J_2 is perpendicular to the prism–sample interface. Because of the symmetry of the apparatus, the reflection spectra at every fixed incident angle θ can be detected. J_1, J_2, and J_3 form a triangle. s, a, and b are the lengths of J_1J_2, J_1J_3, and J_2J_3, respectively. θ can be calculated from

$$\theta = \arccos\left(\frac{b^2 + s^2 - a^2}{2bs}\right). \tag{1}$$

Thus, different θ can be obtained by changing s. Calibrated by the n_r value of water obtained from Ref. 5, any s can be calculated by $s = s_r + s_w$, where s_w is the reference length at the critical angle of water and s_r is the relative length movement of the slider. To determine the internal reflectance spectra at the prism–sample interface, reflection spectra measurement is performed twice in the same angle range. One is for the sample, and the other is for air. Each reflection spectra measurement takes about 5 min. Then the internal reflectance at a fixed θ and a fixed wavelength can be calculated from $R_{\theta,\lambda} = R_{\text{sample}}/R_{\text{air}}$, where R_{sample} and R_{air} are the reflection intensities of the sample and the air, respectively. A similar way to determine the reflectance can be found in Ref. 10, and the difference is that we can obtain the reflectance curve of every wavelength in the continuous spectral region.

Fitting the reflectance curve based on the Fresnel formula[1] is a useful approach to determine the CRI. For the transverse electromagnetic (TE) wave, the reflectance R_{TE} at the prism–sample interface is given by

$$R_{\text{TE}} = \left[\frac{n_p \cos\theta - (u_2 + iv_2)}{n_p \cos\theta + (u_2 + iv_2)}\right]^2. \tag{2}$$

For the transverse magnetic wave, the reflectance R_{TM} is given by

$$R_{\text{TM}} = \left\{\frac{[n_r^2(1-\kappa^2)\cos\theta - n_p u_2]^2 + (2n_r^2\kappa\cos\theta - n_p v_2)^2}{[n_r^2(1-\kappa^2)\cos\theta + n_p u_2]^2 + (2n_r^2\kappa\cos\theta + n_p v_2)^2}\right\}^2, \tag{3}$$

where n_r and κ represent the real part and the imaginary part of CRI of the sample, and n_p is the n_r of the prism. The RID of the prism (made of F4 glass) is according to the values provided in Ref. 18. The prism is made of F4 glass. u_2 and v_2 are the two parameters that satisfy

$$2u_2^2 = n_r^2(1-\kappa^2) - n_p^2\sin^2\theta + \sqrt{[n_r^2(1-\kappa^2) - n_p^2\sin^2\theta]^2 + 4n_r^4\kappa^2}, \tag{4}$$

$$2v_2^2 = -[n_r^2(1-\kappa^2) - n_p^2\sin^2\theta] + \sqrt{[n_r^2(1-\kappa^2) - n_p^2\sin^2\theta]^2 + 4n_r^4\kappa^2}. \tag{5}$$

According to the results in Ref. 11, the CRI of biotissue slightly depends on the polarization of light, so we used unpolarized light as the light source. Then the reflectance R can be calculated as $R = (R_{TE} + R_{TM})/2$.

A nonlinear fitting program based on the Nelder–Mead simplex method[18] was utilized to solve the n_r and κ simultaneously. The consistency between the measured curve and fitting curve is described by E^2, defined as

$$E^2 = 1 - \sum_{i=1}^{N} (R_{m,i} - R_i)^2 / \sum_{i=1}^{N} (R_{m,i} - \bar{R})^2, \quad (6)$$

where $R_{m,i}$ is the ith measured reflectance, R_i is the ith calculated reflectance, and $\bar{R}$ is the mean value of measured reflectance over N values of incident angle. The value of E^2 ranges from 0 to 1, and it is closer to 1 when a reliable fitting is obtained. When n_r and κ at all measured wavelengths are calculated, the continuous CRID of the sample is obtained. The consistency between the measured RID and its fitted dispersion curve are also described by E^2, but here $R_{m,i}$ is the ith measured n_r, R_i is the ith calculated n_r, and $\bar{R}$ is the mean value of measured n_r over N values of wavelengths.

In order to prove the feasibility of the CCRIDM-IR, we made a comparison between the $n_r\kappa$ values of the MR solution determined by CCRIDM-IR and the values obtained from absorption spectra measurement. For MR solution, $\mu_s \approx 0$, so $n_r\kappa$ can be easily deduced from its absorption coefficient by $n_r\kappa = \mu_a\lambda/4\pi$.

3 Result and Discussion

3.1 *Results of Materials with Anomalous Dispersion*

Taken as examples, the reflectance curves of MR solution at the wavelengths of 432.0, 532.1, 632.9, and 732.2 nm are shown in Fig. 2(a), and their fitting coefficients E^2 are 0.996, 0.999, 0.999, and 0.996, respectively. For all measured wavelengths, E^2 values are better than 0.980, indicating that the measured reflectance curves are well fitted. In Fig. 2(b), the CRID of MR solution is demonstrated. Results show that the anomalous dispersion of n_r is well determined, and the values of $n_r\kappa$ match well with the values calculated from absorption spectra measurement. Hence, the feasibility of the CCRIDM-IR method for continuous CRID measurement is proved.

The next group of CRID results is of the hemoglobin solutions. Different from the MR solution, the hemoglobin has more complicated absorption bands and RIDs, as shown in Fig. 3. The absorption bands and the dispersion shape are different when the hemoglobin is oxygenated or deoxygenated. First, both the Hb and HbO_2 have a strong absorption peak in the 400- to 450-nm range, while the peak of Hb is at the longer wavelength. Second, there are two small absorption peaks around 550 nm for HbO_2, while only one peak can be observed for Hb. These results are the same as those in Ref. 19. Zhernovaya et al.[17] have investigated the RI of 320 g/l hemoglobin solution at several discrete wavelengths, and the values are also listed in Fig. 3. Good agreements can be observed. However, it can be found that the discrete RI values cannot provide enough information about the complicated RID of hemoglobin solution. Hence, continuous CRID measurement is necessary.

3.2 *Results of Biotissues with Normal Dispersion*

In this section, several biotissues with normal dispersion were investigated. Taken as examples, reflectance curves of chicken liver at the same four wavelengths are demonstrated in Fig. 4(a). Their E^2 are 0.990, 0.999, 0.992, and 0.998, respectively, and for all measured biotissues, the E^2 is better than 0.980. Unlike MR solution and hemoglobin solution samples, the n_r of chicken liver continuously decreases with the increase of wavelength, and so do the other biotissues, as shown in Figs. 4(b) and 5. This downward trend of n_r has been observed by Bolin et al.[4] To some extent, we can treat this kind of RID as normal dispersion.

From the reflectance curves, the extinction coefficients of biotissue can also be determined. Taken as examples, the extinction coefficient spectra of chicken liver and bovine muscle are shown in Fig. 4(b). Unlike the MR solution and hemoglobin solution samples, no obvious absorption band can be found in the measured spectral range, and the values of κ do not change much with wavelengths. For simplicity, we used the average value of κ as representative, detailed in Table 1.

3.3 *Dispersion Coefficients of Biotissues*

Investigations of the appropriate dispersion equation to describe the RID of biotissues have been made by several researchers.[2,15] Here, we selected

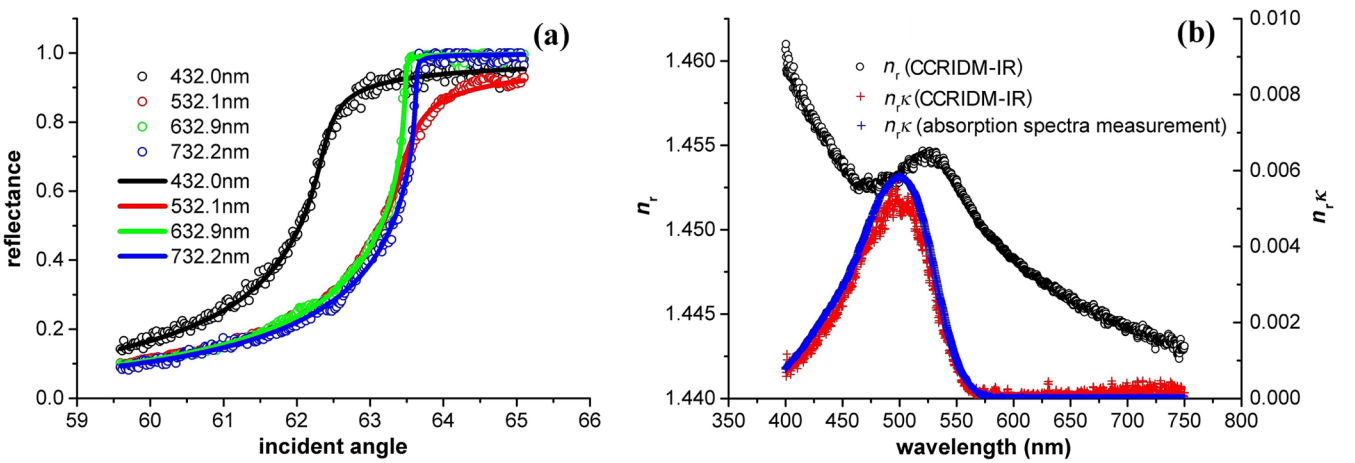

Fig. 2 (a) The experimental and fitted reflectance curves of the MR solution sample; (b) continuous CRID curve of the MR solution sample.

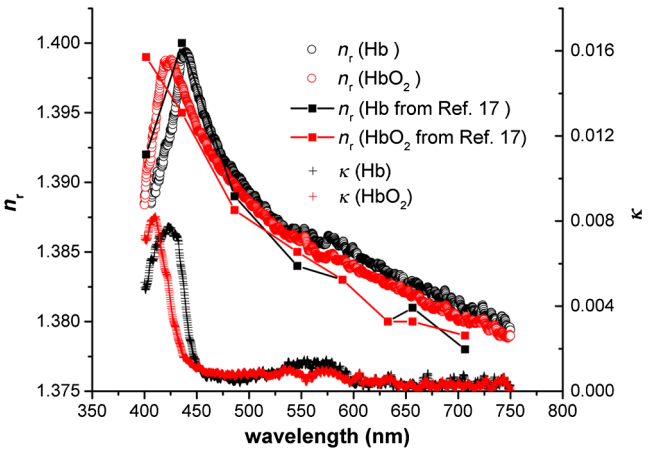

Fig. 3 The CRIDs of deoxygenated (black) and oxygenated (red) bovine hemoglobin at the concentration of 320 g/l.

the Cauchy equation,

$$n_r = A + B/\lambda^2 + C/\lambda^4, \tag{7}$$

the Cornu equation,

$$n_r = A + B/(\lambda - C), \tag{8}$$

and the Conrady equation,

$$n_r = A + B/\lambda + C/\lambda^{3.5}, \tag{9}$$

just as Ding et al. did in Ref. 3. In all the three equations, λ is the wavelength in nanometers. Based on the same nonlinear fitting program, the dispersion coefficients A, B, and C were calculated. Examples of Cauchy equation fitted RID curves of the chicken liver and bovine muscle are demonstrated in Fig. 4 (b). The detailed fitted dispersion coefficients and fitting coefficients of all the measured biotissues are listed in Tables 1–3, respectively. The fitting coefficients are better than 0.970. We also found that for different dispersion equations, the values of the fitting coefficients are close. Hence, all the three chosen dispersion equations are appropriate for the biotissues' RID.

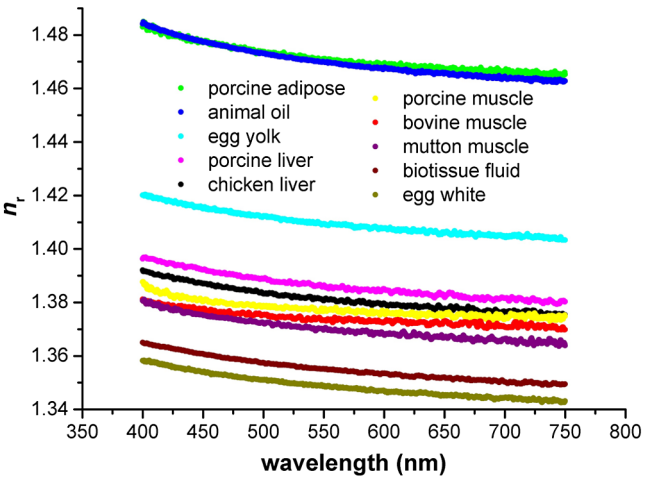

Fig. 5 The RID curves of the biotissue samples with normal dispersion.

3.4 *Discussion*

Results of the same kind of materials show good agreement with each other. Thus, one of the RID curves was chosen as a representative. Since the n_r values of biotissue are often available at several wavelengths in references, comparisons are only made at 632.8 nm to prove the validity of the results, detailed in Table 4, from which we find good agreement between our results and the references.

Results from the continuous CRID measurement of the MR solution also prove that the CCRIDM-IR method can accurately determine the extinction coefficients. For muscle, based on the μ_a and μ_s values from Ref. 20, μ_t is calculated as about 90.37, 84.25, and 74.08 cm^{-1} at wavelengths of 500, 600, and 700 nm, respectively. At the same wavelengths, the μ_t of bovine muscle in this study is calculated as about 120.9, 100.6, and 86.1 cm^{-1}, respectively. The differences of biotissue source and measuring method may be responsible for the mismatches. Hemoglobin is a component that can affect the absorption spectra of muscle. However, in muscle, scattering is much stranger than absorption (e.g., μ_a: 1.17 cm^{-1} and μ_s: 89.2 cm^{-1} at 500 nm as provided in Ref. 20). Hence, the scattering dominates the trend of the κ

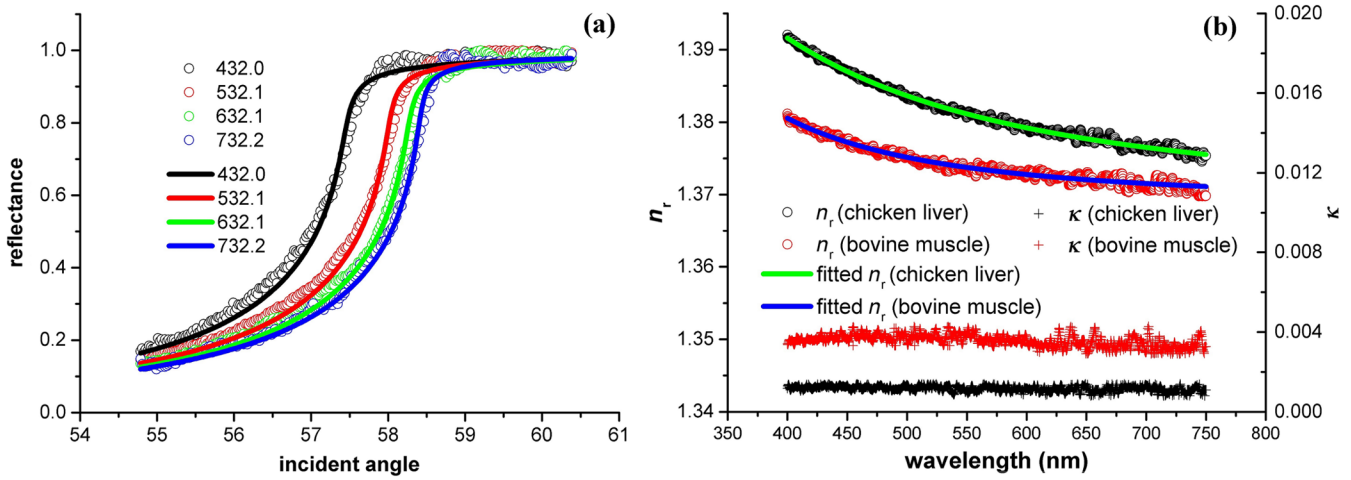

Fig. 4 (a) The experimental and fitting reflectance curves of the chicken liver sample; (b) the measured continuous CRID of chicken liver sample and bovine muscle sample.

Table 1 The coefficients of the Cauchy equation and the average extinction coefficients of biotissues.

Biotissues	A	B	C	E^2	Average κ
Porcine adipose	1.45978	2.83095×10^3	1.53151×10^8	0.996	0.0035 ± 0.0008
Animal oil	1.45506	4.25886×10^3	6.19694×10^7	0.999	0.0005 ± 0.0001
Egg yolk	1.39742	3.66689×10^3	-2.10620×10^6	0.997	0.0004 ± 0.0001
Porcine liver	1.37318	4.04931×10^3	-4.16708×10^7	0.994	0.0010 ± 0.0003
Chicken liver	1.36911	3.67937×10^3	-1.01200×10^7	0.995	0.0012 ± 0.0003
Porcine muscle	1.37307	2.84565×10^2	2.70401×10^8	0.974	0.0038 ± 0.0008
Bovine muscle	1.36827	1.32813×10^3	1.00089×10^8	0.970	0.0035 ± 0.0008
Mutton muscle	1.35922	3.16928×10^3	2.41585×10^7	0.991	0.0047 ± 0.0008
Biotissue fluid	1.34233	4.13473×10^3	-8.48026×10^7	0.998	0.0001 ± 0.00003
Egg white	1.33637	3.97327×10^3	-7.73729×10^7	0.998	0.0001 ± 0.00003

curve, and this is also the reason why the measured κ did not change much with different wavelengths.

Based on the results from both Fig. 5 and Table 1, we can draw the following conclusions. Porcine adipose and animal oil have similar RID values, while the κ of animal oil is much smaller. The extraction process of animal oil can reduce the RI mismatches. The n_r differences between liver samples and muscle samples are not obvious, while the κ of liver samples is smaller. Even though egg yolk and egg white are from the same egg, the n_r of egg yolk is much larger. The high n_r reveals that egg yolk has a high concentration of nutrients. The n_r and κ of biotissue fluid are smaller than those of bovine muscle. We also find that among the muscle samples, mutton muscle has the largest κ and bovine muscle has the smallest values. The theoretical explanation of this phenomenon is being investigated.

The downward trend in n_r of biotissue samples has been observed by Bolin et al.[4] A similar phenomenon can also be found in Ref. 14. To obtain the continuous RID of biotissue, fitting the dispersion equation is a common method. However, using the same nonlinear fitting program to fit the Cauchy equation with the discrete values provided in Ref. 14, we found that the fitting coefficient is only about 0.9. Therefore, the accuracy of the fitting cannot be guaranteed, and whether the Cauchy equation is suitable to describe the RID of biotissue also needs to be verified. However, all these questions have been answered in the current study (Tables 1–3).

3.5 *Error Analysis*

Good agreement between the results in our measurement and references indicates that the CCRIDM-IR is a suitable method for continuous CRID research. The lab-made apparatus provides a tool to measure the angle-dependent internal reflectance spectra of the scattering material. This advantage ensures the CCRIDM-IR method efficiently measures the continuous CRID of biotissue. The error of n_r mainly originates from

Table 2 The coefficients of the Cornu equation.

Biotissues	A	B	C	E^2
Porcine adipose	1.45619	4.71521	228.085	0.996
Animal oil	1.45017	6.97496	195.186	0.999
Egg yolk	1.39323	6.13756	173.762	0.997
Porcine liver	1.36843	6.99616	154.748	0.994
Chicken liver	1.36445	6.52406	160.757	0.995
Porcine muscle	1.37112	1.45705	301.464	0.977
Bovine muscle	1.36648	2.25818	239.963	0.971
Mutton muscle	1.35370	6.67278	143.095	0.991
Biotissue fluid	1.35177	6.36134	170.401	0.998
Egg white	1.33869	6.35775	160.249	0.998

Table 3 The coefficients of the Conrady equation.

Biotissues	A	B	C	E^2
Porcine adipose	1.45640	5.54824	1.69195×10^7	0.996
Animal oil	1.44914	9.21166	1.53730×10^7	0.999
Egg yolk	1.39211	8.17248	9.99411×10^6	0.997
Porcine liver	1.36703	9.29818	8.55509×10^6	0.994
Chicken liver	1.36368	8.28945	9.46374×10^6	0.995
Porcine muscle	1.37381	−0.6151	1.67204×10^7	0.974
Bovine muscle	1.36671	2.54915	9.46621×10^6	0.970
Mutton muscle	1.35458	7.07144	9.94188×10^6	0.992
Biotissue fluid	1.35051	8.53216	9.75361×10^6	0.998
Egg white	1.33583	9.71656	6.19735×10^6	0.998

Table 4 RI of biotissues at 632.8 nm in the current study and in the literature.

Biotissues	Measured	Reference 4	Reference 9	Reference 11	Reference 15
Porcine adipose	1.467	—	1.4699	1.468	—
Chicken liver	1.376	1.380	1.3952	—	–
Porcine muscle	1.376	–	—	1.367	1.379

the calculated incident angle θ. The lengths of a and b are designed to be 160 and 90 mm. J_2 should coincide with the semicircular arc center of the prism, and J_1J_2 is supposed to be perpendicular to the sample–prism interface. Any deviation will cause the error of θ, and the calculation is complex. In Ref. 16, we have measured the RID of K9 glass using the same apparatus, and the results show that the n_r discrepancy is less than 0.0008. Thus, we estimate that the error of n_r in this study is less than 0.001. Because the wavelength interval is only about 0.259 nm, the difference of κ between several adjacent wavelengths should theoretically be very small. So the shift of κ ($\Delta\kappa$) can represent the uncertainty for each continuous CRID measurement. The $\Delta\kappa$ in this study is ± 0.0003 for liver samples, ± 0.0008 for porcine adipose, ± 0.0008 for muscle samples, ± 0.0001 for animal oil and egg yolk, and ± 0.00003 for biotissue liquid and egg white, respectively. For different measurement, the offset of the κ curve is much less than $\Delta\kappa$.

4 Conclusion

It has been a challenge to measure CRID over a continuous spectral region. In this study, CCRIDM-IR is proposed as an approach to study the continuous CRID of biotissues. The feasibility is verified experimentally by our measurements. Continuous CRID values in the spectral region the 400 to 750 nm provide adequate information on the RID and extinction coefficient spectra. To our knowledge, this is the first time that continuous CRID of biotissue with scattering is measured. Improvements can be made by changing the light source, spectrometer, and prism for different application fields.

Acknowledgments

The authors thank the Chinese National Key Basic Research Special Fund (Grant No. 2011CB922003), the Natural Science Foundation of China (Grant Nos. 61475078 and 61405097), the Science and Technology Program of Tianjin (Grant Nos. 15JCQNJC02300 and 15JCQNJC02600), and the International Science and Technology Cooperation Program of China (Grant No. 2013DFA51430).

References

1. M. Bom and E. Wolf, *Principles of Optics*, Pergamon Oxford, Pergamon (1980).
2. H. Ding et al., "Refractive indices of human skin tissues at eight wavelengths and estimated dispersion relations between 300 and 1600 nm," *Phys. Med. Biol.* **51**(6), 1479 (2006).
3. L. Wang, S. L. Jacques, and L. Zheng, "MCML—Monte Carlo modeling of light transport in multi-layered tissues," *Comput. Methods Programs Biomed.* **47**(2), 131–146 (1995).
4. F. P. Bolin et al., "Refractive index of some mammalian tissues using a fiber optic cladding method," *Appl. Opt.* **28**(12), 2297–2303 (1989).
5. M. Daimon and A. Masumura, "Measurement of the refractive index of distilled water from the near-infrared region to the ultraviolet region," *Appl. Opt.* **46**(18), 3811–3820 (2007).
6. D. K. Sardar and L. B. Levy, "Optical properties of whole blood," *Lasers Med. Sci.* **13**(2), 106–111 (1998).
7. G. J. Tearney et al., "Determination of the refractive index of highly scattering human tissue by optical coherence tomography," *Opt. Lett.* **20**(21), 2258–2260 (1995).
8. Q. W. Song et al., "Modified critical angle method for measuring the refractive index of bio-optical materials and its application to bacteriorhodopsin," *J. Opt. Soc. Am. B* **12**(5), 797–803 (1995).
9. J. Lai et al., "Experimental measurement of the refractive index of biological tissues by total internal reflection," *Appl. Opt.* **44**(10), 1845–1849 (2005).
10. M. McClimans et al., "Real-time differential refractometry without interferometry at a sensitivity level of 10^{-6}," *Appl. Opt.* **45**(25), 6477–6486 (2006).
11. Q. Ye et al., "Measurement of the complex refractive index of tissue-mimicking phantoms and biotissue by extended differential total reflection method," *J. Biomed. Opt.* **16**(9), 097001 (2011).
12. H. J. Wei et al., "Determination of optical properties of normal and adenomatous human colon tissues in vitro using integrating sphere techniques," *World J. Gastroenterol.* **11**(16), 2413–2419 (2005).
13. S. C. Gebhart, W. C. Lin, and A. Mahadevan-Jansen, "In vitro determination of normal and neoplastic human brain tissue optical properties using inverse adding-doubling," *Phys. Med. Biol.* **51**(8), 2011 (2006).
14. M. Hammer et al., "Optical properties of ocular fundus tissues—an in vitro study using the double-integrating-sphere technique and inverse Monte Carlo simulation," *Phys. Med. Biol.* **40**(6), 963 (1995).
15. S. Cheng et al., "Measurement of the refractive index of biotissue at four laser wavelengths," *Proc. SPIE* **4916**, 172 (2002).
16. Z. C. Deng et al., "Continuous refractive index dispersion measurement based on derivative total reflection method," *Rev. Sci. Instrum.* **86**(4), 043101 (2015).
17. O. Zhernovaya et al., "The refractive index of human hemoglobin in the visible range," *Phys. Med. Biol.* **56**(13), 4013–4021 (2011).
18. J. A. Nelder and R. Mead, "A simplex method for function minimization," *Comput. J.* **7**(4), 308 (1965).
19. O. Sydoruk et al., "Refractive index of solutions of human hemoglobin from the near-infrared to the ultraviolet range: Kramers–Kronig analysis," *J. Biomed. Opt.* **17**(11), 115002 (2012).
20. A. M. Nilsson, R. Berg, and S. Andersson-Engels, "Measurements of the optical properties of tissue in conjunction with photodynamic therapy," *Appl. Opt.* **34**(21), 4609–4619 (1995)

Zhichao Deng is a PhD student in the Nankai University of Tianjin, China. He graduated in the School of Physics from the same university in 2011. Now, he is mainly engaged in research on biomedical photonics. He has about five years of experience in the study of tissue refractive index.

Jin Wang received her master's degree in biomedical engineering in 2007 and then joined the School of Physics, Nankai University, China. She received her PhD in optics from Nankai University, China, in 2013. Her research interests include optical clearing, refractive index measurement of biotissue, and optical coherence tomography.

Qing Ye received his PhD in optics from Nankai University, China, in 2008 and then joined the School of Physics, Nankai University. Since 2010, he has been an associate professor of optics at the Nankai University. His specialization includes optical coherence tomography, optical clearing, and optical properties measurement of biotissue.

Tengqian Sun completed his bachelor's degree in the School of Physics from Nankai University, China, in June 2011. Currently, he is studying for a doctor's degree in the School of Physics from Nankai University. His PhD studies cover the refractive index microimaging of biomedical, waveguides, and nonlinear materials. He has four years of experience in optical imaging.

Wenyuan Zhou received his master's degree and doctoral degree in 1996 and 2002, respectively. From 2003 to 2012, he worked as an associate professor in the Nankai University. Since 2012, he has been a professor of optics in the Nankai University. His main researches are high sensitive photon detection, photon imaging technology, and application of biological sensor.

Jianchun Mei completed his master's degree in the School of Physics from Nankai University, China, in 2010. The same year, he became an engineer and started to work in the Advanced Technology Institute, Nankai University. He is mainly engaged in the research of photoelectric detection and optical instrument design.

Chunping Zhang has been a professor of physics in the Nankai University since 1995. His main researchers are optical properties and applications of photochromic materials and biomedical photonics.

Jianguo Tian received his PhD from the Nankai University in 1991 and then started to teach in the same university as an assistant professor. In 1995, he became a professor. Since 2001, he has become a specially appointed professor at the Nankai University. He is mainly engaged in condensed matter physics and photonics, involving optical nonlinear mechanism and application of photoelectric material properties.